Rate Studies on Polyaniline Films Preparation in Static Cells and in Fluidized Bed Electrode Reactors

S. SEGELKE,* R. MAHALINGAM,*† and R. V. SUBRAMANIAN,‡
Washington State University, Pullman, Washington 99164

Synopsis

Aniline was polymerized using a static electrochemical cell and a fluidized bed electrode reactor (both static and fluidized beds) to form thin films, respectively, on plate and particulate substrates. Parameters such as reaction time, applied voltage, anolyte flowrate, and monomer concentration on the rate of polymerization were studied and correlated with polymer film thickness and surface morphology, as observed on a scanning electron microscope.

INTRODUCTION

The variety of possible applications for polyaniline (PA), due to its unique physical and electrical properties, has led to an impressive amount of research. Polyaniline can be formed by chemical[1] or electrochemical[2] oxidation, and the latter method can involve organic[3] or aqueous solutions.[4-7] Depending on the conditions the polymer has been subjected to, PA may act as an insulator, a semiconductor, or even a metal-like conductor.[8] The drastic changes in conductivity are due to the combined effects of oxidation and protonic acid doping.[9] Because of this ability to transform PA back and forth between its conducting and insulating forms, PA has been tested for use in microelectronic devices,[10] for corrosion protection of electrodes,[11] and for use in rechargeable batteries.[12] Other investigations have focused on the effects the chemical transformations have on the electrical conductivity,[13] the molecular structure,[14] the reaction mechanism,[15] the molecular weight distribution,[16] and even the fractal dimension.[17]

Much of the kinetic studies on aniline polymerization has been performed using standard electrochemical cells[18] and rotating disk electrodes.[19] The standard cell can be affected by any mass transfer limitations inherent to the system being studied, while experiments using rotating disk electrodes are better able to demonstrate the effects of mass transfer on the reaction rate. A fluidized bed electrode should also be useful for such demonstrations, but few have discussed using such an electrode for electropolymerization.[20,21] A fluidized bed system presents two distinct advantages: (i) The continuous disturbance of the bed contributes to the preferred high rates of mass transfer to the surface

* Department of Chemical Engineering.
† To whom correspondence should be addressed.
‡ Department of Mechanical and Materials Engineering.

Journal of Applied Polymer Science, Vol. 40, 297–312 (1990)
 CCC 0021-8995/90/1-20297-16$04.00

of the particle substrates; (ii) low current densities are made available in view of the large electrode surface per unit volume of the bed. In the work presented here, a fluidized bed electrode reactor (FBER) was used for the electropolymerization of aniline, in an attempt to form conductive films on the particle surfaces. Next, the rate of formation of PA in the fluidized bed reactor was studied and compared with results obtained from static bed experiments. Preparative studies in a standard electrochemical cell (static cell) are also presented for additional comparison.

BACKGROUND

Because of its unique properties, most of the research on PA has attempted to evaluate its physical properties, including: mechanical strength,[14] electrical conductivity,[9,13] spectroscopic absorption,[7] chemical stability,[1] molecular weight,[16] spectral behavior,[22] surface structure,[17] etc. Some work has also been done to demonstrate the possible uses of PA in actual working devices such as rechargeable batteries,[12] electrochromic displays,[23] electrode modifiers,[11] separation membranes,[24] microelectronic devices,[10] etc. The biggest challenges, however, are the reaction mechanism and molecular structures which are still not well understood.

One of the first notable mechanisms for the electrochemical preparation of PA postulates the rate limiting step to be the intermediate formation of the nitrenium cation.[2] Another suggestion is the head-to-head and tail-to-tail coupling of aniline molecules.[25] It has also been noted that cationic mechanisms do not present the only possible means for the polymerization of aniline, as a free radical mechanism is also thought to be possible.[26]

It is believed that the oxidation of aniline to form PA consumes two electrons (e^-'s) per monomer unit, but the number of e^-'s consumed by the polymerization reaction is greater than 2. Genises and Tsintavis,[19] for example, have demonstrated that a maximum of 2.6 e^-'s per monomer unit were consumed during the polymerization of aniline. The extra 0.6 e^-'s are attributed to a reduction-oxidation scheme, with different ratios of imine nitrogen atoms to amine nitrogen atoms creating five distinct forms of PA. It is the transition between these forms which is attributed to the three-state switching effect.

Another form of PA is formed when the polymer film is said to be overoxidized. This usually involves polymerization potentials greater than 0.75 V vs. SCE, and results in the formation of an insulating form of PA, PAH. Even forms of PA which are produced at lower potentials, PAL, can be converted into PAH if subjected to an increased electrical potential which forces additional oxidation. It is assumed to be the formation of crosslinkages, probably involving reactions at the ortho positions, which prevents transformation of PAH back to one of the other forms of PA.[27]

The preparation of polyaniline can be performed many ways. The most common method uses an electrochemical cell to oxidize aniline in either an aqueous[4-7] or an organic solution.[3] Conductive films can be produced in electrochemical cells, with cyclic voltametry creating more homogenous films than potentiostatically formed films.[28] Another method being tested is one which uses a plasma cell,[29] with aniline being vaporized in an inert gas (argon) and deposited anodically on an electrode.

EXPERIMENTAL

Materials

Gold films and graphite particles were used as the working electrodes in the static cell and fluidized bed electrode reactor (FBER), respectively.

Conductive gold tape (3M Company) has a thin layer of Au sandwiched between a mylar film and an adhesive backing. The adhesive backing was used to stick the tape to one face of a glass microscope slide, and the mylar coating was dissolved in phenol. A piece of insulated copper wire, with the insulation stripped from both ends, was used to pass current to the Au tape.

The graphite particles used were prepared by cutting with a band saw $\frac{1}{8}$ in. (3.2 mm) diameter machined graphite rods, produced by the National Electrical Carbon Corporation. The graphite rods had a density of 1.8 g/cm^3 and a specific resistance of 10.0 $\mu\Omega$ m. The average length of the particles was 4.46 mm.

Reagent grade aniline (Fisher Scientific) was distilled for use in the polymerization experiments. Reagent grade hydrochloric acid (Baker Chemical) and phenol (Baker Chemical) were used without further purification.

Static Cell Experiments

The initial experiments used two of the three compartments of a stationary cell. The compartments of the cell were separated by two porous sintered glass discs. The cathode compartment contained 250 mL of 3.0 *M* aqueous HCl and used a platinum plate for the cathode. A strip of one-inch-wide gold tape, stuck to one face of a glass microscope slide, served as an anode while partially immersed in an aqueous 1.0 *M* aniline/3.0 *M* HCl solution. The potential difference between the gold tape and a saturated calomel electrode (SCE) placed in the anode compartment, and the current flow between the gold anode and the platinum cathode, was continuously measured. Next, experiments were performed in this cell by systematically varying the applied cell potential, the reaction time, and the solution concentrations. The standard reaction conditions used the previously described solutions with a constant 2.0 V potential difference maintained between the Au tape and the Pt cathode for a period of 7 min. The exposed surface area of the gold tape was either 1.0 cm^2 or 0.75 in.^{2} depending upon the experiment. The potential was varied from 0.5 to 3.5 V, the reaction time was varied from 5 to 50 min, the acid concentration was varied from 0.75 to 4.5 mol/L, and the monomer concentration was varied from 0.2 to 1.5 mol/L. The amount of polymer deposited was obtained by weighing and the film thickness from scanning electron microscopy (SEM). A Perkin-Elmer Fourier transform infrared (FTIR) spectrometer using KBr disks established the absorbance bands for PA. Conductivity measurements using the four-point probe technique were carried out on $\frac{1}{2}$ in. diameter PA disks prepared by stripping the PA off the gold tape, grinding it to a fine powder and compacting under a 2000 lbf for 2 min.

Particle Bed Electrode Experiments

The particle bed electrode experiments were done potentiostatically between a bed of graphite particles which performed as the anode, and a platinum cath-

ode. With these experiments the effects of reaction time, aniline concentration, applied voltage, and anolyte flowrate were examined. The ranges over which the time, concentration, and voltage were varied are the same as those stated for the static cell. The anolyte flow rate was varied from 0 to 1.5 L/min, giving a bed expansion in the range of 0–20%. The experiments were carried out in a dual compartment cell made of polysulfone, with a concentric configuration as shown in Figure 1. The two compartments were separated by a porous alundum thimble. A perforated Teflon disk supported the particles and acted as a flow distributor. Together, the reactor stands 11 in. tall with an external diameter of $3\frac{3}{8}''$. The internal diameter of the center compartment (anode compartment) is $1\frac{1}{2}$ in. The anode was a bed of cylindrical graphite particles weighing about 8 g with a bed porosity of 0.56 ± 0.02. Current fed to the particles passed through a graphite rod which was made of the same material as the particles. The rod was coated, except at the ends, with polyurethane in order to reduce its reactive surface area, leaving only 188 mm^2 of the rod surface exposed to the solution. A reference (SCE) electrode was also used in the anode com-

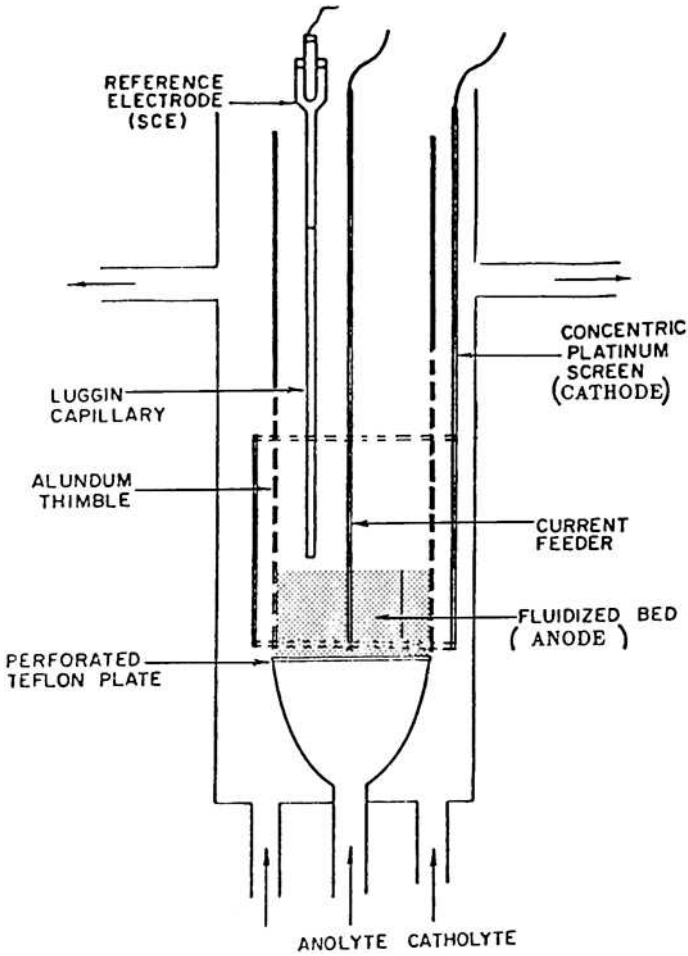

Fig. 1. Fluidized bed electrode reactor.

partment as shown in Figure 1; the cathode was a cylindrical platinum screen placed in the outer compartment. The potential difference between graphite particles and the SCE, and the current flow through the reactor, were continuously measured using strip chart recorders which were connected as in the static cell experiments.

The solutions used in both compartments were circulated by corrosion-resistant pumps through flowmeters, glass heat exchangers, and stainless steel valves, as shown in Figure 2. The anolyte was a 2-L aqueous solution of 0.8 *M* aniline and 1.85 *M* HCl. The catholyte was a 2-L aqueous 2.0 *M* hydrochloric acid solution. The anolyte was used mainly at three flow conditions. The first was no flow, creating a static bed condition. The second provided enough flow so that the particles could move only slightly, but not rise. This incipient fluidization condition used a flow rate of 0.8 L/min. A third flow rate of 0.85 L/min forced the particles to rise and expand the bed height by about 20%. Our previous studies[20,21] had shown that 15–20% fluidization should provide the optimum conditions when using a fluidized bed electrode. The catholyte flow rate was maintained at either 0 or 0.6 mol/min for the static bed and fluidized bed experiments, respectively.

The amount of PA formed was established, as before, by weighing. SEM pictures provided information on film thickness and surface morphology.

RESULTS AND DISCUSSION

The multistep mechanism for the autocatalytic electropolymerization of aniline does not avail itself to a kinetic study which would be able to test the

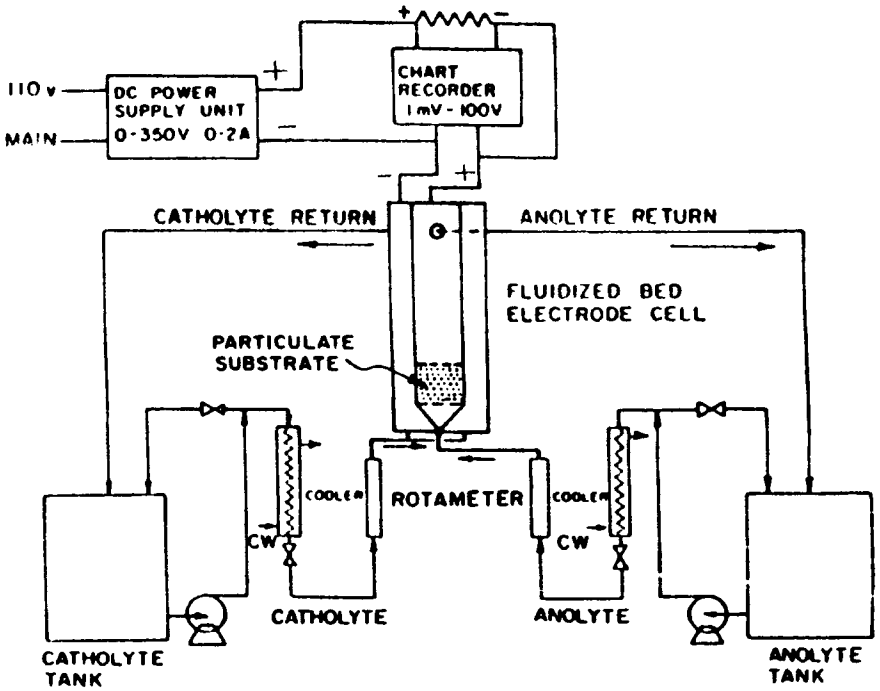

Fig. 2. Flow setup for fluidized bed electrode reactor.

mechanism directly using an integral method. Instead, the effects of rate determining factors need to be examined independently using a differential method, like the method of excess. It is expected that charge transfer, mass transfer, and reaction temperature would affect the reaction rate, so that factors influencing the behavior of these properties in the polymerization system were examined. Charge transfer is affected by the EMF applied between the two electrodes of the electrochemical reactor and by the amount of charged ions in the reactor solutions. The greater the force exerted on the charged ions, and the greater the number of ions, the greater the rate of charge transfer. In this case, the ions were those created by dissolving both hydrogen chloride and aniline in an aqueous solution. Mass transfer is influenced by the concentration of the reactants, which in this case was aniline, and by the hydrodynamics of the reactor. As the concentration of aniline was increased, the mass transfer of aniline to the reactive surface was expected to improve. In the FBER, the reactant fluid was forced to flow past the reactive surface, providing higher mass transfer rates than in a static bed or cell reactor. In static cases, mass transfer is provided only through diffusional effects and natural convection. Temperature could also have an effect on the reaction rate in electrochemical reactors, but this effect was not studied here. Instead, water-cooled heat exchangers were added to the FBER to insure that the reactant solution was always kept at the same temperature, 23 ± 2°C. The static cell experiments were also run at room temperature.

For a homogeneous reaction in a constant volume reactor, with the reaction occurring at an interface, a reaction rate expression (r) will take the form of

$$r_i = \frac{1}{S}\frac{dN_i}{dt} \tag{1}$$

with S representing the total reactive surface area, N_i representing the moles of component i reacting, and t representing the reaction time. For the polymerization of aniline, the number of moles reacted could only be approximated, because adequate means of monitoring concentration changes of the reactant were not incorporated into the experiments. Only weight measurements and SEM thickness measurements of the PA film deposits were used to show the changes in deposition rates with respect to system changes. PA is insoluble in most solvents, both organic and aqueous, and so it was assumed that all the PA formed was deposited on the anode. However, PA films formed in an aqueous acid solution (like the one used in our experiments) become doped with the acid, so that the weight measurements of the PA film deposits could not be converted to a mole expression for the amount of aniline reacted since the amount of doping is not known. Therefore, the actual rate expression used for the study of aniline electropolymerization had to take the form:

$$r_{\text{an}} = \frac{1}{S}\frac{dM_{\text{PA}}}{dt} \alpha \frac{-1}{S}\frac{dN_{\text{an}}}{dt} \tag{2}$$

which assumes either that the amount of acid in the polymer is considered negligible or that a constant mass concentration of acid is formed in the PA

films. As long as the concentration of acid is kept constant, the amount of doping in the PA films should remain about the same, though voltage changes may affect the doping level. The FBER experiments use a continuously recycled, fixed volume of reactant fluid, so that a batch approximation is appropriate and helps to avoid unnecessary complications of a separate rate expression for a flow process. Thus eq. (2) becomes applicable here also.

The experiments that were performed were done in sets. Each set was used to show the effects of varying each parameter on the overall reaction rate. For the static cell experiments the parameters studied were: aniline concentration, acid concentration, anode surface area, applied electrical potential, and reaction time. The fluidized bed experiments examined only the effects of: anolyte flow rate, aniline concentration, applied electrical potential, and reaction time.

Some of the static cell experiments involved the measurement of the PA film thickness instead of the weight of the polymer deposit. If a constant polymer density is assumed, the film thickness is

$$X = \frac{M_{PA}}{\rho S} \tag{3}$$

Thus,

$$r'_{an} = \frac{dX}{dt} = \frac{1}{\rho S}\frac{dM_{PA}}{dt} = \frac{1}{\rho} r_{an} = \text{coating rate} \tag{4}$$

This constant polymer density assumption may not be valid for experiments involving acid concentration changes or applied voltage changes, since both have been shown to affect the morphology of PA deposits, which would probably change the density of the PA deposits.

Static Cell Experiments

In the initial experiments, effects of the acid concentration on the reaction rate were examined in order to select a range for a detailed study on the FBER. The concentration of HCl in the anode compartment was varied from 0.75 to 6.0 mol/L of anolyte (M); concentrations greater than 1.5 M showed only a slight increase in the coating rate. A large change did occur, however, between 0.75 and 1.5 mol HCl/L where the coating rate jumped from 0.9 to 10.7 μm/min (Fig. 3). Subsequent experiments were limited to this range because the concentration of aniline could not be maintained at 1 M in an acidic solution of less than 0.75 M HCl due to solubility limitations; also, at concentrations of 6 M HCl or greater, the gold tape was consumed soon after the electrical potential was applied to the static cell.

When similar experiments were run with varying concentrations of aniline from 0.2 to 1.5 M, a plot of reaction rate vs. aniline concentration (Fig. 4) showed that the reaction rate peaked near 0.65 M. It is possible that in concentrated solutions the electrical potential attracts too much aniline to the surface of the anode at once. This might cause the aniline in solution near the working electrode to "salt out" if the localized concentration of aniline exceeds the solubility limit of the anolyte solution. This would create a diffusional

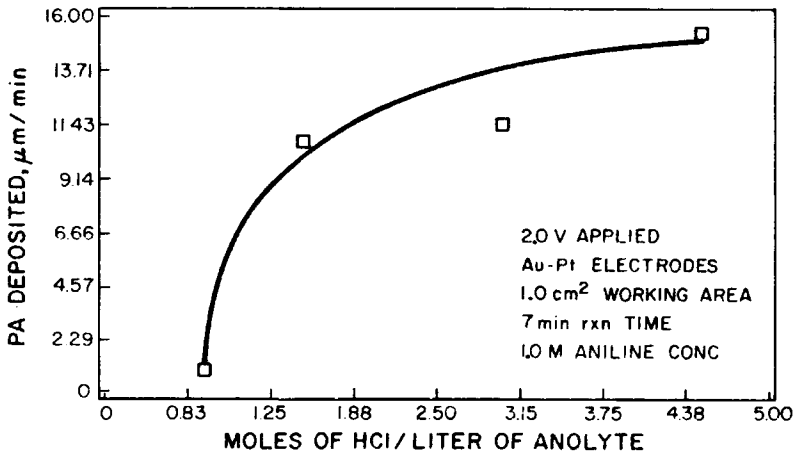

Fig. 3. Coating rate as function of acid concentration (static cell).

barrier limiting the polymerization rate and could explain the peak in the rate curve shown in Figure 4.

The possibility that an overoxidized insulating layer caused the reaction rate to diminish at the higher aniline concentrations was ruled out since the current vs. time plots did not show the characteristic sudden reduction in current flow. In fact, formation of an overoxidized layer, which was described by Thyssen,[15] was only noticed in the experiments which studied the changes in the reaction rate over time (Fig. 5). The current vs. time plots for this set of experiments showed that after the first 5 min the reaction rate stabilized at its maximum value and remained constant until the current flow to the anode essentially stopped in a matter of seconds. In the experiments using 1.0 cm^2 Au electrodes, the reaction was halted about 15 min after it was begun, as shown in Figure 5.

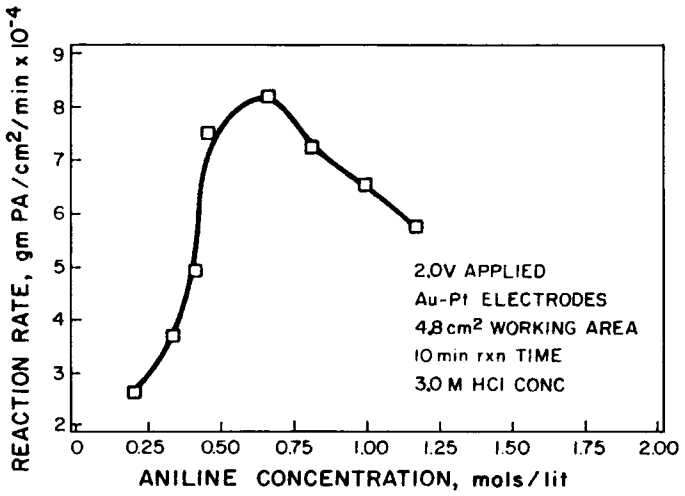

Fig. 4. Reaction rate as function of monomer concentration (static cell).

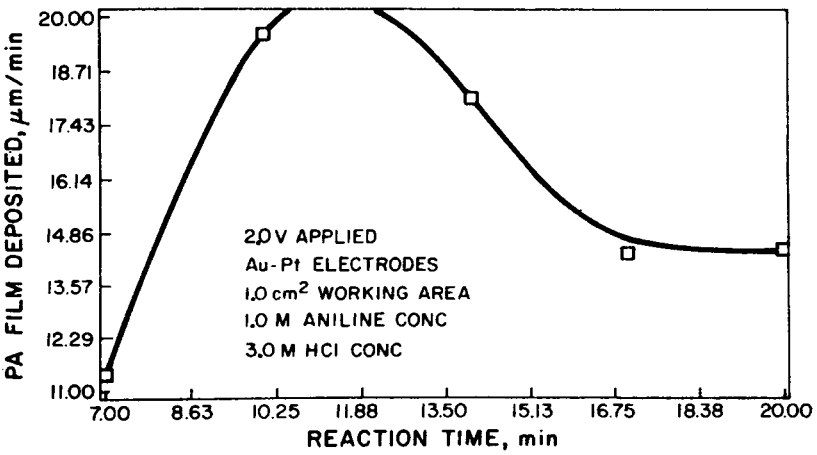

Fig. 5. Coating rate as function of reaction time (static cell).

The experiments using working areas of 4.8 cm^2, however, were not stopped until about 35 min into the reaction (Fig. 6). Therefore, one may assume that since the anode surface area to reactor volume ratio is less with the larger electrodes, the diffusional barrier is not as easily established.

The experiments used to study the effect of electrical potential on the reaction rate also yielded a maximum point on the curve. As shown in Figure 7, the rate peaked near a potential of 2.0 V. Since overoxidation is more likely to occur at the higher potentials, it is probably the partial formation of a nonconductive branched form of PA which hinders the reaction rate when the potential goes above 2.0 V. Also, hydrogen overvoltage appears to hinder the reaction at potentials above 3.0 V. This was suggested by the bubbled nature of the coatings which are formed at these higher potentials.

Since both weight and thickness readings (100–150 μm) were taken, the *in situ* value for the polymer density (formed using a 1.0 *M* aniline/3.0 *M* HCl

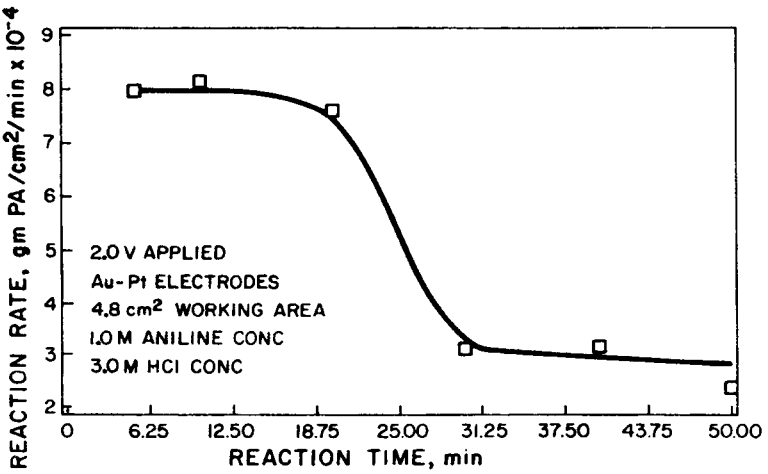

Fig. 6. Reaction rate as function of reaction time (static cell).

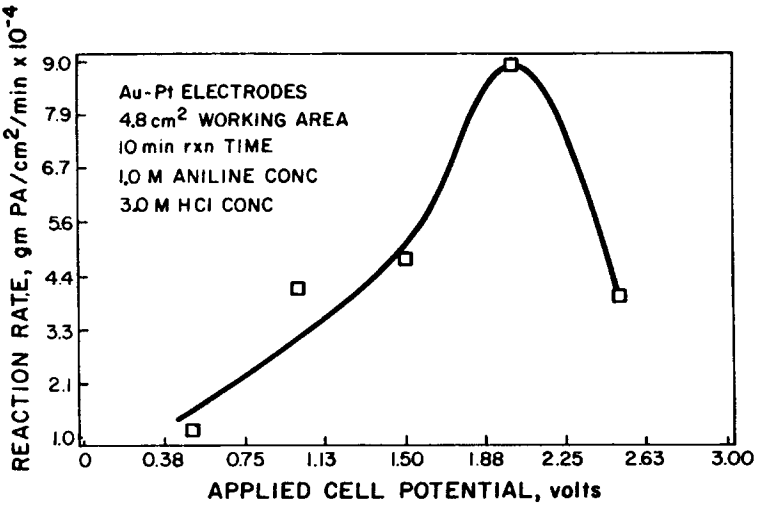

Fig. 7. Reaction rate as function of applied potential (static cell).

solution with a 2.0 V potential difference between the Au tape and the Pt cathode) was calculated to be 0.16 ± 0.02 g/cm^3.

It was also possible to determine the polymerization charge (the number of e^-'s required for one molecule of aniline to polymerize), under the same conditions as were just stated. This required the assumption that no chloride ions were present in the polymer so that the dry weight could be used to estimate the amount of aniline reacted. These calculations showed that 2.1 ± 0.2 electrons were used per monomer reacted. This value is less than the value of 2.2 given by Thyssen et al.,[13] and considerably smaller than the 2.7 derived by Genies and Tsintavis.[15] If chloride ions were still present in the dried polymer, then the estimate of the number of aniline molecules reacted should be lower, forcing the electron to monomer reacted ratio to be larger than 2.1.

Particle Bed Experiments

When the aniline concentration was varied in the fluidized bed reactor, the static bed experiments showed a significant change in the amount of polymer retained on the particles, as is shown in Figure 8. For the two fluidized bed conditions, there is little change possibly due to the polymer deposits being washed off the surface of the particles due to anolyte flow; this will be discussed later. It should be noted, though, that in the static bed (Fig. 8), the peak concentration level has shifted to 1.1 *M* instead of 0.8 *M* as was demonstrated in the static cell (Fig. 4) with Au electrodes. This is probably due to the use of different electrode materials which had different amounts of exposed surface area. The graphite particle bed provided a larger electrode area to reactor volume ratio, which should allow for better transfer of aniline to the electrode surface. The porous graphite surface might also provide better adhesion between PA and the substrate, which could improve charge transfer to the reactive polymer surface.

The peak associated with the applied potential has also shifted. This can be seen in Figure 9. It is presumably the added resistance of the graphite particle

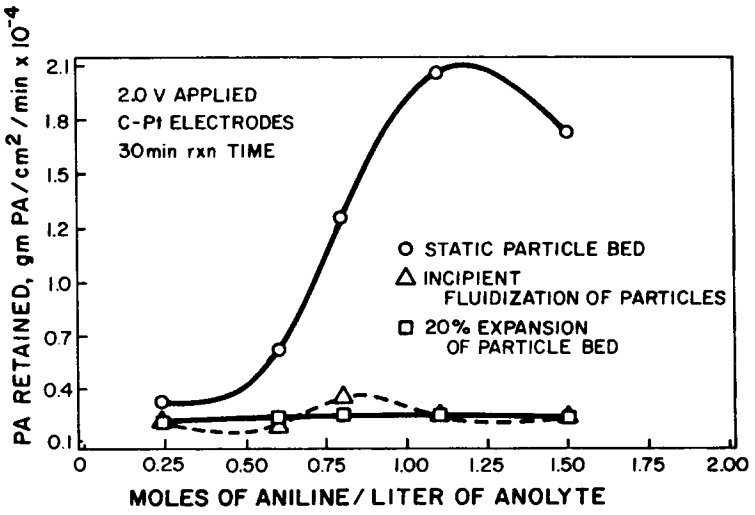

Fig. 8. Reaction rate as function of monomer concentration (fluidized bed reactor).

bed that has caused this shift, since some of the electrical potential will be used to transport the electrons to the particle surfaces. This may also be related to the change in morphology at the various potentials. As the potential increases, the amount of oxidation undergone by the polymer is also increased, so that the transition is gradually made from the conductive form to the insulating form of PA. The set of micrographs, shown in Figure 10, demonstrates this change. It appears that as the potential is increased from 1.4 to 3.5 V, the polymer loses its fine stringy structure and tends to form into a more densely packed structure.

In all of the fluidizing experiments it became apparent that most of the polymer was easily washed off except for the adhering film in direct contact

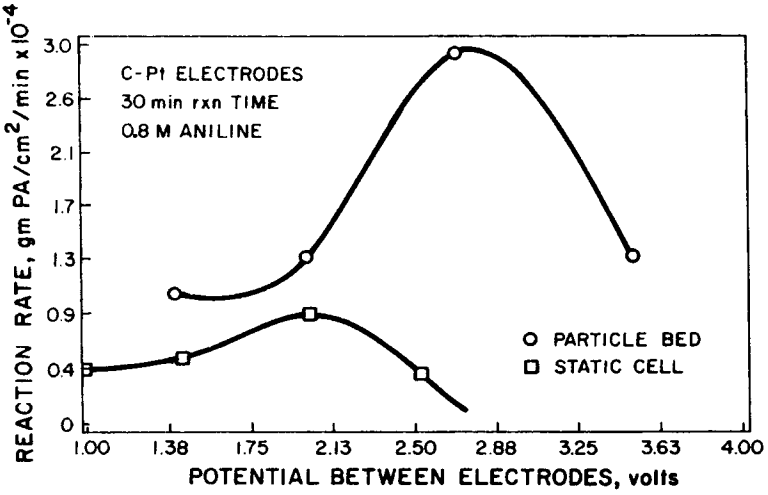

Fig. 9. Reaction rate as function of applied potential (static cell and static bed reactor).

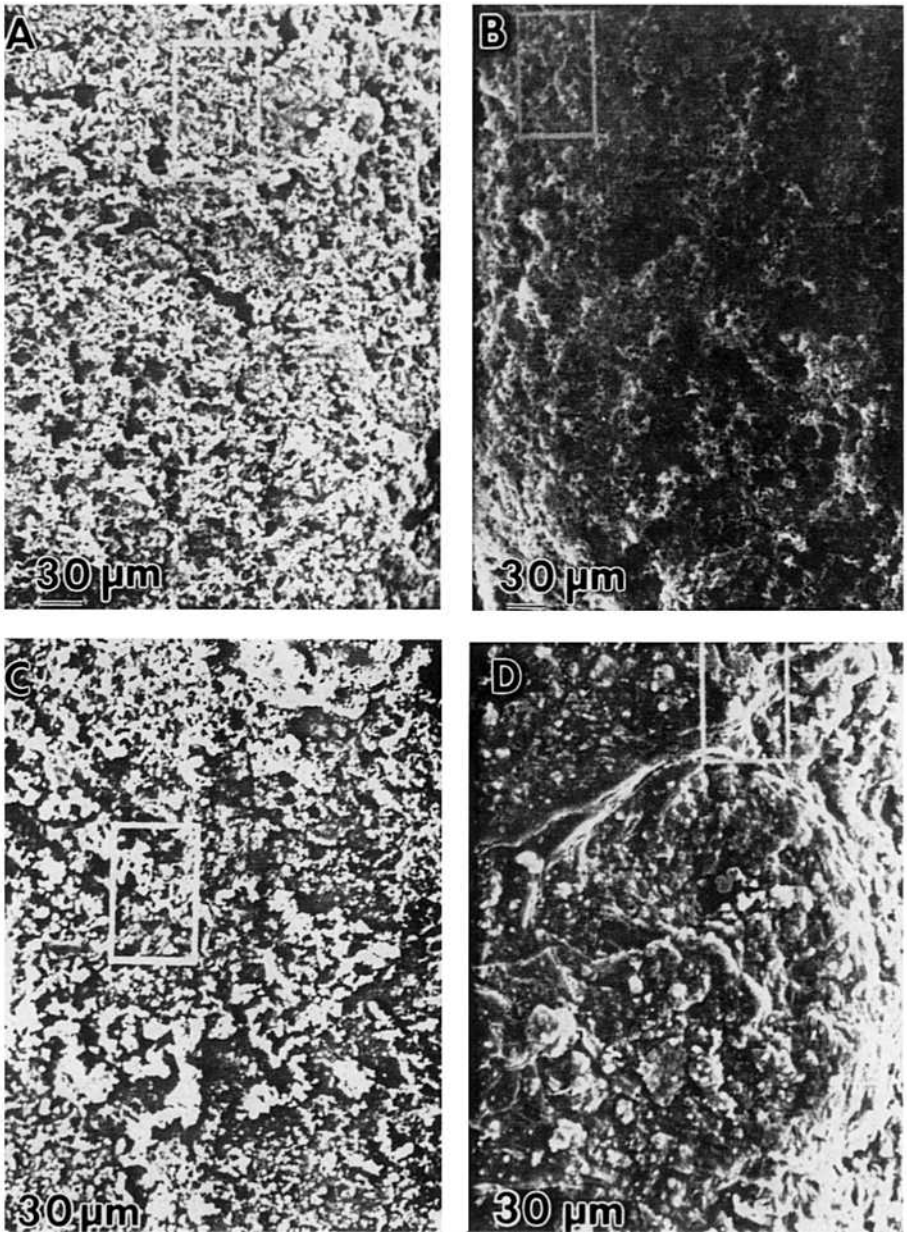

Fig. 10. Effect of varying applied voltage between graphite particle bed and platinum cathode on polymer morphology: (A) 1.4 V; (B) 2.0 V; (C) 2.7 V; (D) 3.5 V.

with the graphite particles. The current consumed in the fluidized runs was about the same as the static bed consumption, as demonstrated in Figure 11; yet less polymer was found coated on the fluidized graphite. Thus, Figures 12, 13, and 14, when plotted as polymer retained as a function of various parameters, in addition to Figure 8, clearly show the wash off. The experiments involving the effect of reaction time on the reaction rate showed that the reaction rate

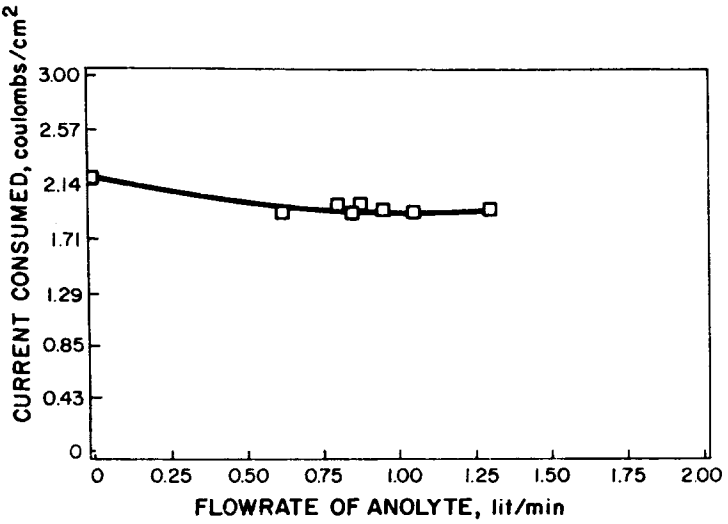

Fig. 11. Consumed current as function of anolyte flow rate (fluidized bed reactor).

tended to increase slightly with time in the static bed and stayed constant with time in the fluidized runs (Fig. 14). This was due to the steady wash-off of PA. Since the polymer surface is continuously being removed, it is quite possible that the overoxidized insulating layer, which eventually inhibits the reaction in a static cell, will never form. The current vs. time plots support this assumption by showing a steady flow of current throughout the experiments, without the eventual sudden reduction seen in the static cell tests.

CONCLUSIONS

In the static cell experiments the rate limitations of high aniline concentrations (> 0.7 *M*), long reaction time (> 30 min), and high voltages (> 2.0 V

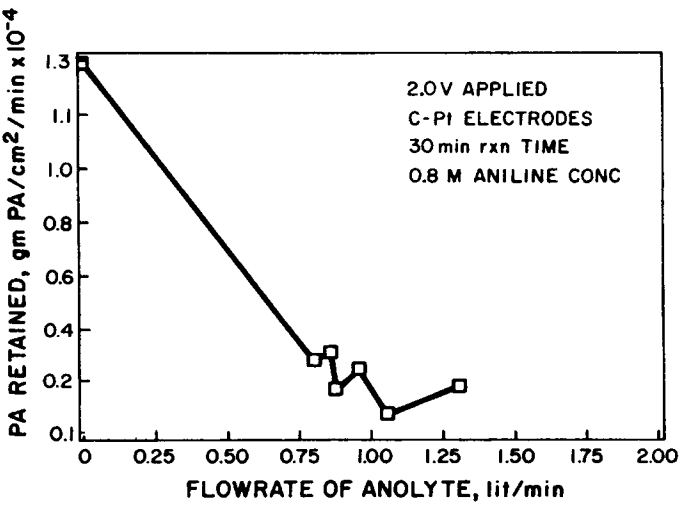

Fig. 12. Reaction rate as function of anolyte flow rate (fluidized bed reactor).

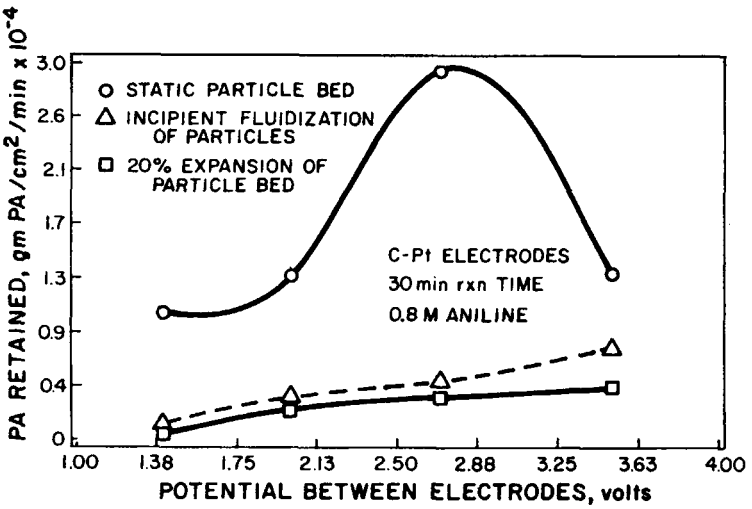

Fig. 13. Reaction rate as function of applied potential (fluidized bed reactor).

between Au and Pt) were demonstrated. At high aniline concentrations a diffusional barrier was assumed to be formed due to the salting out effect. When the reaction period was long enough, a nonconductive film eventually coated the electrode and prevented further polymerization. At high voltages also the reaction was hindered by the formation of a nonconductive film. The limiting effects of these parameters were similarly demonstrated in static particle bed experiments.

The above limitations were not encountered in the fluidized bed experiments since most of the PA film formed in the particle bed was removed by anolyte flow past the particles. The amount of current drawn for the polymerization

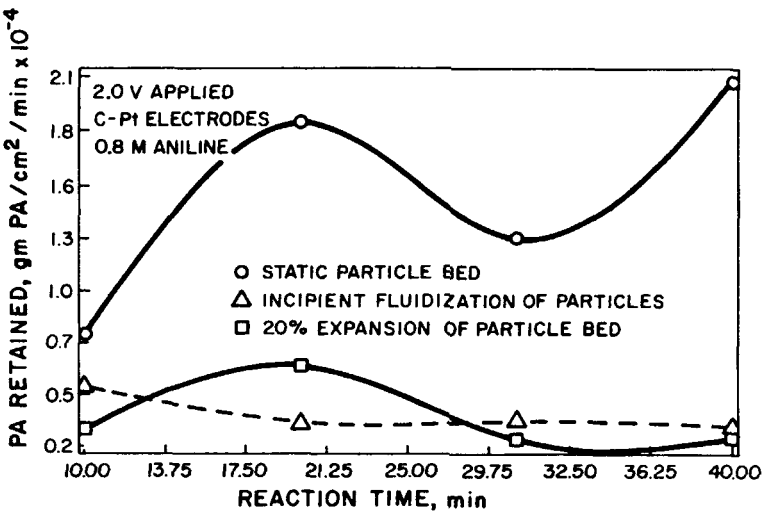

Fig. 14. Reaction rate as function of reaction time (fluidized bed reactor).

of aniline in the fluidized bed experiments was, however, as much as was drawn in the static bed experiments. This implies that as much PA was being produced in the fluidized bed experiments as was produced in the static bed experiments, even though most of the PA was not collected as a film deposit.

It was mentioned previously that a rate limiting effect occurs over time due to the formation of an insulating film layer. The constant removal of polymer film from the particles in the FBER may prevent the formation of the non-conducting layer, thus allowing for a steady reaction rate in the FBER. Thus, although the polymer remaining on the surface of the particles is less than the deposits from static bed experiments, the fluidized bed electrode may be advantageous in a production operation since polymer could be produced and peeled off at a constant rate as an anolyte suspension and collected by filtering or settling operations.

The surface structure of the PA films observed with a SEM showed the effects of varying the reaction time, electrical potential and aniline concentration. As the reaction time increased, a more uniform and complete coating of both the Au tape in the static cell experiments and the graphite particles in the static bed experiments was shown. Increased potential showed its effects in static cell and static bed experiments as well by demonstrating that porous structures were formed at lower potentials, and smoother, less porous structures were formed as the potential was increased. The effects of changing the aniline concentration, however, seemed to be negligible in both the static cell and particle bed runs.

Portions of this research were supported with funds from National Science Foundation Grant #CBT-8519001.

APPENDIX: NOMENCLATURE

M_{PA}	mass of polyaniline film (g)
N_i, N_{an}	moles of species i and aniline, respectively, (g mol)
r_i	reaction rate of species i (g mol/cm^2 min)
r_{an}	reaction rate of aniline (g/cm^2 min)
r'_{an}	deposition rate of aniline (μm/min)
S	total reactive electrode surface area (cm^2)
t	reaction time (min)
X	polymer film thickness (μm)
ρ	density of dried polymer film (g/cm^3)

References

1. A. G. Macdiarmid, S. H. Mu, N. L. D. Somasiri, and W. Wu, *Mol. Cryst. Liq. Cryst.*, **121**, 187–190 (1985).

2. D. M. Mohilner, R. N. Adams, and W. J. Argersinger Jr., *J. Am. Chem. Soc.*, **84**, 3618–3622 (1962).

3. K. A. Macor, Y. O. Su, L. A. Miller, and T. G. Spiro, *Inorg. Chem.*, **26**, 2594–2598 (1987).

4. N. Oyama, Y. Ohnuki, K. Chiba, and T. Ohsaka, *Chem. Lett.*, 1759–1762 (1983).

5. R. Holze, *J. Electroanal. Chem.*, **224**, 253–260 (1987).

6. C. M. Carlin, L. J. Kepley, and A. J. Bard, *J. Electrochem. Soc.*, **132**, 353–359 (1985).

7. T. Ohsaka, Y. Ohnuki, and N. Oyama, *J. Electroanal. Chem.*, **161**, 399–405 (1984).

8. A. G. Macdiarmid, J. C. Chiang, M. Halpern, W. S. Huang, S. L. Mu, N. L. D. Somasiri, W. Wu, and S. I. Yaniger, *Mol. Cryst. Liq. Cryst.*, **121**, 173–180 (1985).

9. P. M. McManus, R. J. Cushman, and S. C. Yang, *J. Phys. Chem.*, **91**, 744–747 (1987).

10. E. W. Paul, A. J. Ricco, and M. S. Wrighton, *J. Phys. Chem.*, **89**, 1441–1447 (1985).

11. G. Mengoli, M. T. Munari, P. Bianco, and M. M. Musiana, *J. Appl. Polym. Sci.*, **26**, 4247–4257 (1981).

12. A. G. Macdiarmid, A. Kitani, M. Kaya, and K. Sasaki, *J. Electrochem. Soc.*, **133**(6), 1069–1073 (1986).

13. A. Thyssen, A. Borgerding, and J. W. Schultze, *Makromol. Chem. Macromol. Symp.*, **8**, 143–157 (1987).

14. A. Kitani, M. Kaya, S. I. Tsujiaka, and K. Sasaki, *J. Polym. Sci. Polym. Chem. Ed.*, **26**, 1531–1539 (1988).

15. E. M. Genies and C. Tsintavis, *J. Electroanal. Chem.*, **195**, 109–128 (1985).

16. A. Watanabe, K. Mori, Y. Isasaki, and Y. Nakamura, *J. Chem. Soc. Chem. Commun.*, **1**, 3–4 (1987).

17. B. Villeret and M. Nechtschein, *Solid State Commun.*, **63**(4), 435–437 (1987).

18. A. F. Diaz, *Makromol. Chem. Macromol. Symp.*, **8**, 17–37 (1987).

19. E. M. Genies and C. Tsintavis, *J. Electroanal. Chem.*, **200**, 127–145 (1986).

20. R. Mahalingam, F. S. Teng, and R. V. Subramanian, *J. Appl. Polym. Sci.*, **22**, 3587–3596 (1978).

21. F. S. Teng and R. Mahalingam, *J. Appl. Polym. Sci.*, **34**, 2837–2852 (1987).

22. W. Huang, B. D. Humphrey, and A. G. MacDiarmid, *J. Chem. Soc.*, **82**, 2385–2400 (1986).

23. M. P. Albert and J. F. Combs, *IEEE Trans. Electron Devices*, **11**, 148–151 (1964).

24. R. L. Hand and R. F. Nelson, *J. Electrochem. Soc.*, **125**, 1059–1963 (1978).

25. M. Breitenbach, and K. H. Heckner, *Electroanal. Chem. Interfacial Electrochem.*, **43**, 267–286 (1973).

26. S. Glasstone, *The Fundamentals of Electrochemistry and Electrodeposition*, Franklin, Palisades, NJ, 1960.

27. A. Kitani, M. Kaya, J. Yano, K. Yoshikawa, and K. Sasaki, *Synth. Metals*, **18**, 341–346 (1987).

28. A. Diaz and J. A. Logan, *J. Electroanal. Chem.*, **111**, 111–114 (1980).

29. M. Inoue, H. Fujioka, T. Sorita, and T. Tanaka, *Polym. Prepr. Am. Chem. Soc., Div. Polym. Chem.*, **28**(2), 332–333 (1987).

Received October 18, 1988
Accepted April 6, 1989